PAPER

Anti-inflammatory activity of *Sanghuangporus sanghuang* by suppressing the TLR4-mediated PI3K/AKT/mTOR/IKKβ signaling pathway

Wang-Ching Lin,[a] Jeng-Shyan Deng,[b] Shyh-Shyun Huang,[a] Wan-Rong Lin,[c] Sheng-Hua Wu,[d] Hui-Yi Lin[a] and Guan-Jhong Huang [ID] *[c]

Sanghuangporus sanghuang (SS) is a mushroom that belongs to the genus *Sanghuangporus* and it is commonly called "Sangwhang" in Taiwan. It is popular in oriental countries and has been traditionally used as food and medicine. The mystery surrounding it was solved in 2012, when it was discovered. However, existing research has not extensively investigated the anti-inflammatory effect of sanghuang that grows on *Morus* trees. The aim of this study is to investigate the protective effects and underlying mechanism of SS on inflammation by lipopolysaccharide (LPS) induced *in vitro* and *in vivo*. Results showed that SS treatment markedly attenuated LPS-induced lung edema, by elevation of the levels of interleukin (IL)-1β, tumor necrosis factor (TNF)-α and IL-6 in bronchoalveolar lavage fluid (BALF) accompanied by a remarkable improvement of lung histopathological symptoms. Additionally, western blotting results suggest that anti-inflammatory effects of SS against the LPS-induced ALI may be due to its ability to inhibit the PI3K/Akt/mTOR/IKK, NF-κB and MAPK signaling pathways. Notably, our results suggest that SS suppresses LPS-induced ROS by inducing Nrf2 activation and HO-1, thioredoxin-1 expression in the lung tissues. Moreover, these findings suggest a potential application of SS in pulmonary inflammatory disease therapy.

1. Introduction

The respiratory system is often exposed to dust and airborne pathogens, and respiratory epithelial tissue clears foreign pathogens through activation of the immune response, thereby maintaining health.[1] However, a common cause of respiratory tract inflammation is infection caused by Gram-negative bacteria, which contain endotoxins in their cell membrane; endotoxins irritate the respiratory tract, thereby triggering an immune response.[2] This attracts neutrophils and macrophages that accumulate in lung tissue as a means to clear pathogens. However, leukocytes take a long time to infiltrate the lung tissue, which not only delays the time taken to relieve the inflammatory response, but also causes increasingly serious damage to the lung tissue.[1,2] Acute lung inflammation results in lung damage, referred to as acute lung injury (ALI). ALI is a common but serious lung disease that in severe cases, can easily lead to acute respiratory distress syndrome (ARDS) and sepsis, both of which have high mortality rates.[2,3] Thus far, no effective treatment for ALI is available.[3]

Lipopolysaccharide (LPS), a component of the cell membrane of Gram-negative bacteria, is a common environmental endotoxin. Toll-like receptor 4 (TLR4) is the receptor for LPS.[4] When LPS binds to TLR4 expressed in respiratory epithelial cells, the downstream signaling pathways nuclear factor-κB (NF-κB) and mitogen-activated protein kinase (MAPK) are activated by myeloid differentiation factor 88 (MyD88), causing alveolar macrophages to secrete large amounts of pro-inflammatory cytokines.[5] These cytokines cause neutrophils in the peripheral blood vessels to migrate and gather in the alveolar and interstitial space, where large amounts of free radicals and reactive oxygen species (ROS) are released as a means to kill the foreign pathogens.[6] However, this release can also damage the surrounding alveolar epithelium, resulting in pulmonary interstitial edema, disruption of the alveolar epithelial barrier, and leakage of large amounts of protein into the alveoli, consequently resulting in serious lung damage.[4–7]

Phosphatidylinositol 3-kinase (PI3K) and its downstream target protein kinase B (also known as Akt), Akt can influence cell survival and are relevant to lipopolysaccharide (LPS)-induced signal transduction. Akt can regulate nuclear factor (NF)-κB activation caused by LPS. By promoting IκB kinase (IKK) for NF-κB phosphorylation, Akt can increase the transcription

[a] School of Pharmacy, China Medical University, Taichung 404, Taiwan. E-mail: linwc0913@gmail.com; sshuang@mail.cmu.edu.tw; hylin@mail.cmu.edu.tw

[b] Department of Health and Nutrition Biotechnology, Asia University, Taichung 413, Taiwan. E-mail: dengjs@asia.edu.tw

[c] School of Chinese Pharmaceutical Sciences and Chinese Medicine Resources, College of Chinese Medicine, China Medical University, Taichung 404, Taiwan. E-mail: linwr0627@gmail.com; gjhuang@mail.cmu.edu.tw

[d] Department of Biology, National Museum of Natural Science, Taichung 404, Taiwan. E-mail: shwu@mail.nmns.edu.tw

ability of NF-κB.[8] Moreover; Akt can regulate the activity of mechanistic target of rapamycin (mTOR). A recent study showed that after phosphorylation by Akt, mTOR can bind to and phosphorylate IKK in order to promote NF-κB activation.[8,9] Inhibition of mTOR can reduce LPS-induced production of pro-inflammatory cytokines and NF-κB phosphorylation.[9] This indicates that the route for PI3K/Akt/mTOR/IKK signal transduction has an essential impact on NF-κB activation.[8–10]

Many studies have reported numerous inflammatory substances and excessive oxidative stress in ALI patients.[11] To determine an effective treatment for ALI, one must first identify a medication that can inhibit inflammation in the lungs and suppress excess oxidative stress in the body.[12]

The use of *Sanghuangporus sanghuang* (abbreviated in this article as SS or sanghuang), a valuable medicinal fungus, has been widespread in China, Japan, and Korea for more than a millennium. The mystery surrounding it was solved in 2012, when it was discovered by Wu *et al.*[13,14] Being extremely rare, genuine sanghuang is distributed throughout mainland China, Japan, South Korea, and Taiwan; and it only grows on mulberry (*Morus*) trees in the wild.

A recent study reported that sanghuang has moderate pharmacological activity: it enhances immunity, antitumor,[15,16] anti-inflammatory,[16–18] antioxidant activity;[16–18] and hepatoprotective effects;[19] among others. According to a research report, the active compounds in the sanghuang fruiting body include polysaccharides, triterpenoids, pyran and furan ketones, and polyphenolic compounds.[20] However, existing research has not extensively investigated the anti-inflammatory effect of sanghuang that grows on *Morus* trees.

Therefore, the aim of this study was to investigate whether sanghuang that grows on *Morus* trees has an anti-inflammatory ability, through both *in vitro* and *in vivo* experiments: one using endotoxin-induced macrophage cells, and the other using an endotoxin-induced ALI mouse model to assess the anti-inflammatory capacity of sanghuang and investigate its possible mechanism.

2. Materials and methods

2.1. Source of material

This study used basidiocarps from sanghuang varieties: *S. sanghuang* grown on *Morus*. Dr Sheng-hua Wu of the Department of Botany of the National Museum of Natural Science, Taiwan kindly identified and supplied varieties.

2.2. Sample extraction

Dried sanghuang powders were immersed in and extracted with 70% ethanol for five days, followed by filtration. Filtrates were concentrated under reduced pressure to remove ethanol. This step was repeated four times to obtain the extracts, which were then stored for subsequent analysis.

2.3. Cell culture

A murine macrophage cell line RAW264.7 (BCRC No. 60001) was purchased from the Bioresources Collection and Research Center (BCRC) of the Food Industry Research and Development Institute (Hsinchu, Taiwan). Cells were cultured in plastic dishes containing Dulbecco's Modified Eagle Medium (DMEM, Sigma, St. Louis, MO, USA) supplemented with 10% fetal bovine serum (FBS, Sigma, USA) in a CO_2 incubator (5% CO_2 in air) at 37 °C and subcultured every 3 days at a dilution of 1 : 5 using 0.05% trypsin–0.02% EDTA in Ca^{2+}-, Mg^{2+}-free phosphate-buffered saline (DPBS).

2.4. Cytotoxicity and NO, cytokine, ROS production

RAW264.7 cells (5×10^4 cells per well) were cultured in 96-well plate in DMEM containing 10% FBS for 24 h to become nearly confluent. Then cells were cultured with increasing concentrations of SS (125–500 μg mL^{-1}) in the presence of 100 ng mL^{-1} LPS for 24 h. After that, cells were incubated with 100 μL of 0.5 mg mL^{-1} MTT (Sigma, USA) for 4 h at 37 °C. After incubation, the colored formazan crystals formed in culture plate was dissolved in 0.04 N HCl/isopropanol. The optical densities (OD) were measured at 570 nm using a microplate reader (Molecular Devices, USA). The viability of RAW264.7 cells in each well was presented as compared with percentage of untreated control cells.

NO production was indirectly assessed by measuring the nitrite levels in the culture media using Griess reagent assay. Briefly, RAW264.7 cells were seeded at a density of 5×10^4 cells per well in 96-well plates for 24 h. After incubation, the cells were treated with SS (125, 250 and 500 μg mL^{-1}) in the presence of LPS (100 ng mL^{-1}) for 24 h. The culture supernatant was collected for nitrite assay. Each of 100 μL of culture media was mixed with an equal volume of Griess reagent (1% sulfanilamide, 0.1% naphthyl ethylenediamine dihydrochloride and 5% phosphoric acid) and incubated at room temperature for 5 min, the absorbance was measured at 540 nm with a microplate reader (Molecular Devices). Fresh culture media were used as blanks and the nitrite levels were determined by using a standard curve obtained from sodium nitrite.

Macrophages were seeded at 5×10^4 cells per well in 96-well plates. Cells were incubated with SS (125, 250 and 500 μg mL^{-1}) in the presence of LPS (100 ng mL^{-1}) for 24 h. Cell culture supernatants were centrifuged at $5000 \times g$ for 3 min at 4 °C to remove insoluble material. Secreted IL-1β, IL-10, IL-6, and TNF-α were measured in cell culture supernatants using commercially-available ELISA kits (BioLegend, San Diego, CA) following the instructions provided by the manufacturers. The absorbance (450 nm) for each sample was analyzed using microplate reader and was interpolated with a standard curve. Results of three independent experiments were used for statistical analysis.

RAW264.7 cells were seeded at a density of 5×10^4 cells per well in 12-well plates for 24 h. After incubation, the cells were treated with SS (125, 250 and 500 μg mL^{-1}) in the presence of LPS (100 ng mL^{-1}) for 24 h. After 24 h of LPS treatment, DCFH-DA (10 μM) was added for 30 min. Cells were then washed and resuspended in PBS, and fluorescence was measured using Synergy HT Microplate Reader (BioTek Instruments) after excitation at 485 nm and emission at 535 nm. ROS level was expressed as percentage over control. Three replicates were carried out for each of the different treatments.

2.5. Animals

Animals male ICR mice, 6–7 weeks old, were obtained from BioLASCO Taiwan Co., Ltd (Taipei, Taiwan). The animals were kept in plexiglass cages at a constant temperature of $22 \pm 1\ °C$, relative humidity $55 \pm 5\%$ and with 12 h dark–light cycles. They were given food and water *ad libitum*.

Animal studies were conducted according to the regulations of Instituted Animal Ethics Committee, and the protocol was approved by the Committee for the Purpose of Control and Super-vision of Experiments on Animals (Protocol No. 2016-376). After a 1–2 week adaptation period, male ICR mice (25–32 g) were randomly assigned to eight groups ($n = 6$) of the animals in the study. The control group received normal saline (intra-peritoneal, i.p.). The other groups included a LPS-treated (5 mg kg^{-1}), a positive control (LPS + Dex, 10 mg kg^{-1}) and SS administered groups (LPS + SS-L, 125 mg kg^{-1}; LPS + SS-M, 250 mg kg^{-1}; LPS + SS-H 500 mg kg^{-1}). One hour before the intratracheal administration of LPS, the animals received an intravenous injection of 3.0 mg kg^{-1} of TAK-242 (LPS + TAK groups) or co-treatment with SS (500 mg kg^{-1}) and TAK-242 (LPS + TAK + SSH group).

2.6. Model of LPS induced ALI

Seventy-two healthy male ICR mice were randomly divided into 8 groups ($n = 6$): control group, LPS group, dexamethasone (Dex) group (10 mg kg^{-1}), low dosage SS group (125 mg kg^{-1}), middle dosage group (250 mg kg^{-1}, LPS + SS-M) high dosage group (500 mg kg^{-1}, LPS + SS-H), TAK groups (3.0 mg kg^{-1}, LPS + TAK-242) as well as co-treatment with SS (500 mg kg^{-1}) and TAK-242 (3.0 mg kg^{-1}, LPS + TAK + SSH group).

Take half of each group for the inflammation protein analysis, slicing, and edema and the rest of mice use for BALF analysis. Mice were intratracheally instilled with 5 mg kg^{-1} LPS in 50 μL sterile saline or sterile saline alone (control group). In brief, mice were anesthetized with mixed reagent of 10 μL g^{-1} i.p. urethane (0.6 g mL^{-1}) and chloral hydrate (0.4 g mL^{-1}), followed by Dex (10 mg kg^{-1}) or lobeline intraperitoneal injection with individual dose. Six hours later, the mice received sacrifice and bronchoalveolar lavage fluid (BALF) and lung tissues were collected.

2.7. Bronchoalveolar lavage fluid (BALF), total cell count and protein analysis

Six hours later, mice were exsanguinated after anesthesia. According to the previous report, BALF was collected by the upper part of the trachea, by douche three times with 500 μL PBS (pH 7.2). The fluid recovery rate was more than 90%. Lavage sample from each mouse was kept on ice. BALF was centrifuged at $700 \times g$ for 5 min. The sediment cells were resuspended in 2 mL PBS, half of them have used to detect cell counts by cytometer, the rest equally divided into two parts. One has centrifuged again in order to get sediment for extracting proteins with a RIPA solution (radioimmuno-precipitation assay buffer) and centrifuged again to obtain the supernatant in order to detect total protein content by Bradford assay.

2.8. TNF-α, IL-6, and IL-1β cytokines in BALF

Serum levels of TNF-α, IL-1β, and IL-6 were determined using a commercially available enzyme linked immunosorbent assay (ELISA) kit (Biosource International Inc., Camarillo, CA) according to the manufacturer's instruction. TNF-α, IL-1β, and IL-6 were determined from a standard curve.

2.9. Myeloperoxidase (MPO) activity assay

The lungs were homogenized, $12\ 000 \times g$ at 4 °C for 15 min and resuspended in 50 mM KPO$_4$ buffer (pH 6.0) with containing 0.19 mg mL^{-1} of *o*-dianisidine chloride and 0.0005% H$_2$O$_2$ was a substrate for myeloperoxidase at 460 nm with a spectropho-tometer (Molecular Devices, Sunnyvale, CA, USA). MPO content was expressed as relative MPO activity (OD460 nm mg^{-1} protein of lung tissue).

2.10. Lung wet/dry weight ratio

The lower lobe of the left lung was blotted dry and weighed before being placed in an oven at 80 °C for 48 h to obtain the "dry" weight. The ratio of the wet lung weight to the dry lung weight was calculated to assess tissue edema. The right lungs were used for histopathological examination.

2.11. H&E staining

The right lung was harvested and fixed in 10% buffered formalin for 24 h, dehydrated, embedded in paraffin before being stained with hematoxylin and eosin (H&E) and observed under light microscopy.

2.12. Protein extraction and western blot analysis

RAW264.7 cells were seeded at a density of 5×10^6 cells per dish in 10 cm dish and then with different concentrations of SS (125, 250 and 500 μg mL^{-1}) and 100 ng mL^{-1} of LPS for 24 h to measure the protein expression levels. The cells were harvested and lysed by RIPA buffer (Thermo Fisher Scientific, Waltham, MA) for 20 min on ice, and the lysates were centrifuged at $10\ 000 \times g$ for 15 min at 4 °C. Nuclear and cytosolic extracts of the cells were prepared by Nuclear & Cytoplasmic Extraction Kit according to the manufacturer's instructions (G-Biosciences, USA).

PBS and RIPA were added to lung tissue before grinding. The extract was then centrifuged at $12\ 000 \times g$ for 15 min to obtain the supernatant. Bovine serum albumin (BSA) was used as a protein standard to calculate the equal total cellular protein amounts. Protein samples (50 μg) were resolved by denaturing 10% sodium dodecyl sulfate-polyacrylamide gel electrophoresis (SDS-PAGE) using standard methods, and then were transferred to PVDF membranes (Immobilon, Mil-lipore, Bedford, MA, USA) by electroblotting and blocking with 5% skim milk. The membranes were then incubated with mouse monoclonal anti-iNOS, anti-COX-2, anti-NF-κB (p65), anti-IκB, anti-p-IκB, anti-Nrf2, anti-HO-1, anti-MAPK antibody and antioxidative enzymes (SOD, GPx, Catalase, Trx-1) in TBST at 4 °C overnight, washed three times with TBST, and incu-bated for 1 h at 37 °C with horseradish peroxidase conjugated secondary antibodies. The membranes were washed three

times before being detected for immunoreactive proteins with enhanced chemiluminescence (ECL) using hyperfilm and ECL reagent (Thermo, Scientific Hudson, USA). The results of Western blot analysis were quantified by measuring the relative intensity compared to the control by using Kodak Molecular Imaging Software (Version 4.0.5, Eastman Kodak Company, Rochester, NY) and represented in relative intensities.

Antibodies against Nrf2, HO-1, IκB-α, p-IκB-α, NF-κB, P38 and β-actin were obtained from Abcam (Cambridge, UK, USA). Antibodies against iNOS, COX-2, p-ERK1/2, p-JNK, JNK, Trx-1, Keap-1, KAP1, GPX1, CAT, SOD-1, TLR4, AKT and HMGB1 was purchased from Gene Tex (San Antonio, TX, USA). Antibodies against ERK1/2, MPO, IKK, p-IKK and p-mTOR was obtained from Cell Signaling Technology (Danvers, MA, USA). Antibody against p-P38, p-AKT, PI3K was purchased from Millipore (Billerica, MA, USA).

2.13. Fingerprint analysis by HPLC

The analysis will be performed on a HITACHI HPLC L-5000 system equipped with adegasser, pumps, and a photodiode array detector linked to a PC computer running the software program HPLC LACHROM. For HPLC analysis, an aliquot (10 μL) is injected into the columns and eluted at 40 °C. The analytical column (250 × 4.6 mm i.d., 5 μm) used is Thermo Hypersil GOLD C_{18} (USA), and the detection wavelength. For photodiode array detection, the wavelengths of standard compounds at their respective maximum absorbance wavelength can monitored at the same time. Identification is based on retention times and on-line spectral data in comparison with authentic standards.

The mobile phase contained acidified water with acetic acid (2.5%, solvent A) and methanol (solvent B). The gradient program started with 10% solvent B for 0 min, then linearly increased to 20% solvent B for another 5 min. This linear gradient was followed by an isocratic elution until 30 min and reconditioning steps to return to the initial mobile phase condition. The flow rate was 0.8 mL min^{-1}, and the injection volumes of standards and samples were 10 μL.

2.14. Statistical analysis

Unless otherwise stated, all experiments were performed at least three times independently. Experimental results were presented as the mean ± standard deviation (SD) of three parallel measurements. Statistical evaluation was carried out by one-way analysis of variance (ANOVA) followed by Scheffe's multiple range tests. Statistical significance was expressed as #$p < 0.05$, ##$p < 0.01$ and ###$p < 0.001$ were compared with sample of control-alone group; *$p < 0.05$, **$p < 0.01$, and ***$p < 0.001$, were compared with LPS-alone group.

3. Results

3.1. Cytotoxicity and NO inhibition

As shown in Fig. 1, administration of various doses of SS did not affect the viability of murine macrophages, while administration of a nontoxic dose of SS could significantly reduce the levels of LPS-induced nitric oxide (NO) and pro-inflammatory cytokines in macrophages.

3.2. Effects of SS on LPS-induced iNOS, COX-2, NF-κB, MAPK and TLR4/PI3K/Akt/mTOR/IKKβ protein expressions in macrophages

Meanwhile, it was also found that SS could significantly reduce the expression of inducible nitric oxide synthase (iNOS) and cyclooxygenase-2 (COX-2), as shown in Fig. 2A. In SS-administered groups, protein expression levels of cytoplasmic NF-κB p65 and inhibitor of IκBα, along with p-IκBα, decreased. As shown in Fig. 2, LPS-alone group markedly increased the translocation of NF-κB p65 to the nucleus. However, treatment of SS significantly reduced the nuclear translocation of NF-κB p65. Furthermore, SS significantly regulated the phosphorylation of intracellular extracellular signal-regulated kinases 1 and 2 (ERK-1/2), c-Jun n-terminal kinase (JNK 1), and p38 proteins. As shown in Fig. 2C, TLR4 and PI3K protein expression was significantly induced, and Akt and IKKβ protein phosphorylation increased in the LPS-induced group as compared with that reported for the control group. Compared with the LPS group, the SS-administered group showed a significant reduction in the activity of the TLR4/PI3K/Akt/mTOR/IKKβ signaling pathway.

3.3. Effects of SS on LPS-induced antioxidative enzymes, HO-1, Trx-1/Nrf2 proteins expressions and ROS production in macrophage

In terms of antioxidant enzymes in cells, in SS-administered groups, there was a significant increase in intracellular protein expression of glutathione peroxidase (GPX), superoxide dismutase (SOD), catalase (CAT), heme oxygenase-1 (HO-1), thioredoxin-1 (Trx-1) and nuclear factor erythroid-2-related factor (Nrf2) in the cytoplasm, as shown in Fig. 3A.

Thus, we investigated whether SS attenuates LPS-stimulated ROS production. As shown in Fig. 3B, SS treatment significantly reduced LPS-induced ROS production in a dose-dependent manner in RAW 264.7 cells. These findings suggest that the anti-inflammatory effect of SS may be associated with its anti-oxidant effects in RAW 264.7 cell.

3.4. Effects of SS on LPS-mediated lung histopathologic changes

In tissue sections, as shown in Fig. 4, marked alveolar and interstitial thickening as well as edema with leukocyte infiltration was observed in LPS groups. In groups administered SS and DEX prior to LPS induction, alveolar and interstitial edema could be reduced, and leukocyte infiltration could be alleviated, as shown in Fig. 4.

3.5. SS attenuates pulmonary edema and reduces cellular counts and proteins in BALF in LPS-induced ALI mice

Comparisons of wet/dry lung weight ratios, cell numbers and protein concentrations in bronchoalveolar lavage fluid, and
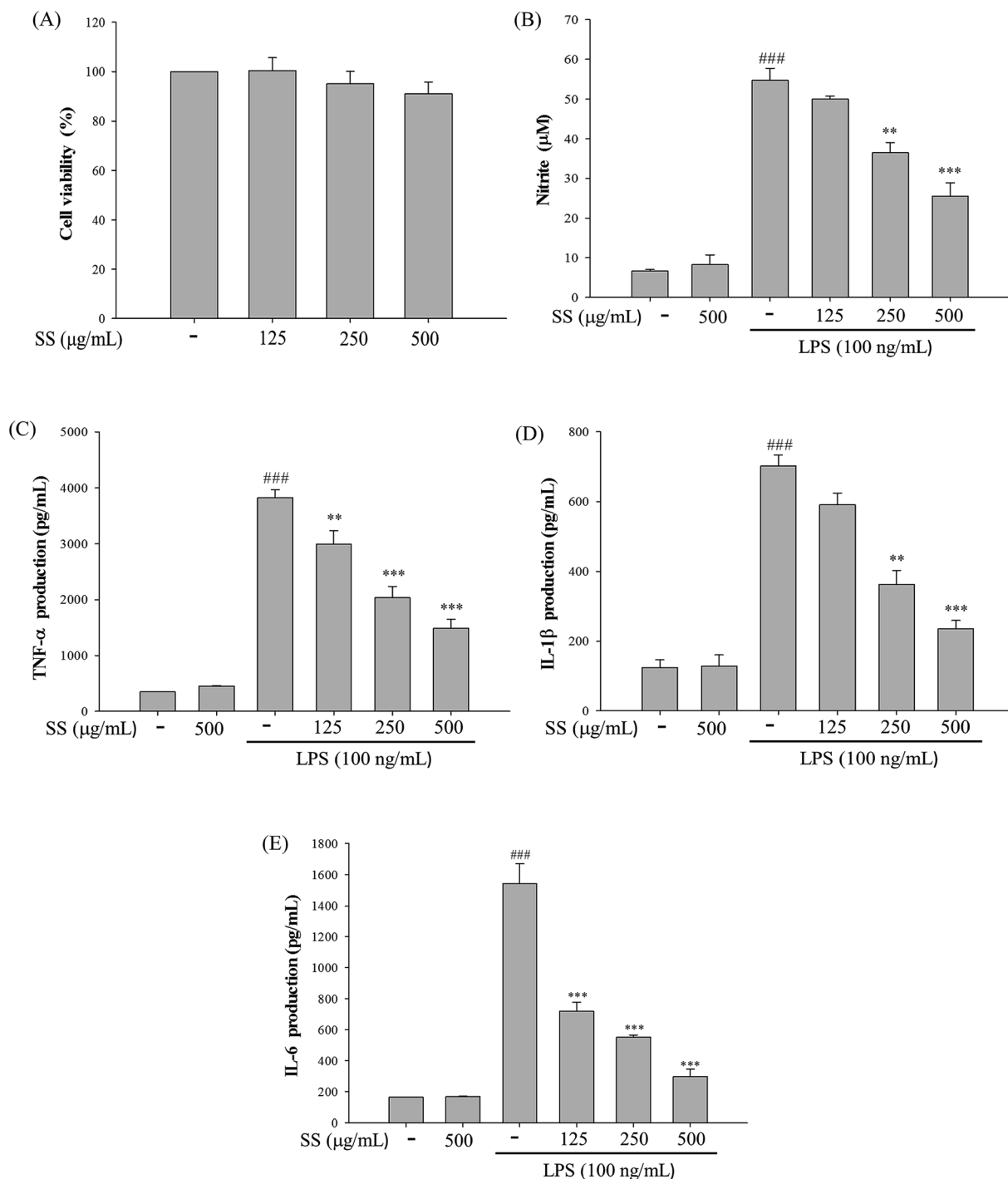
Fig. 1 SS inhibited lipopolysaccharide (LPS)-induced cell inflammation in RAW 264.7 cells. Cytotoxicity (A) of SS in LPS-stimulated RAW264.7 cells. Cells were treated with SS at 125, 250 and 500 μg mL^{-1} for 24 h, and cell viability was assayed by the MTT assay. NO (B), TNF-α (C), IL-1β (D), and IL-6 (E) production in LPS-stimulated RAW264.7 cells. Cells were incubated with or without LPS (100 ng mL^{-1}) in the presence of various doses (125, 250 and 500 μg mL^{-1}) of SS for 24 h. The data were presented as mean ± SD for the three different experiments performed in triplicate. ###$p < 0.001$ were compared with sample of control-alone group (one-way ANOVA followed by Scheffe's multiple range tests). **$p < 0.01$, and ***$p < 0.001$ were compared with LPS-alone group.

lung myeloperoxidase (MPO) activity are shown in Fig. 5. Compared with the control group, the LPS-induced group sowed a significant increase in wet/dry lung weight ratio, cell numbers and protein concentrations in bronchoalveolar lavage fluid, and lung MPO activity. As shown in Fig. 5, a significant

reduction in wet/dry lung tissue weight ratio and MPO activity, as well as cell counts and protein concentrations in bronchoalveolar lavage fluid was observed in groups first administered LPS, as compared with the values reported for the LPS-induced group.
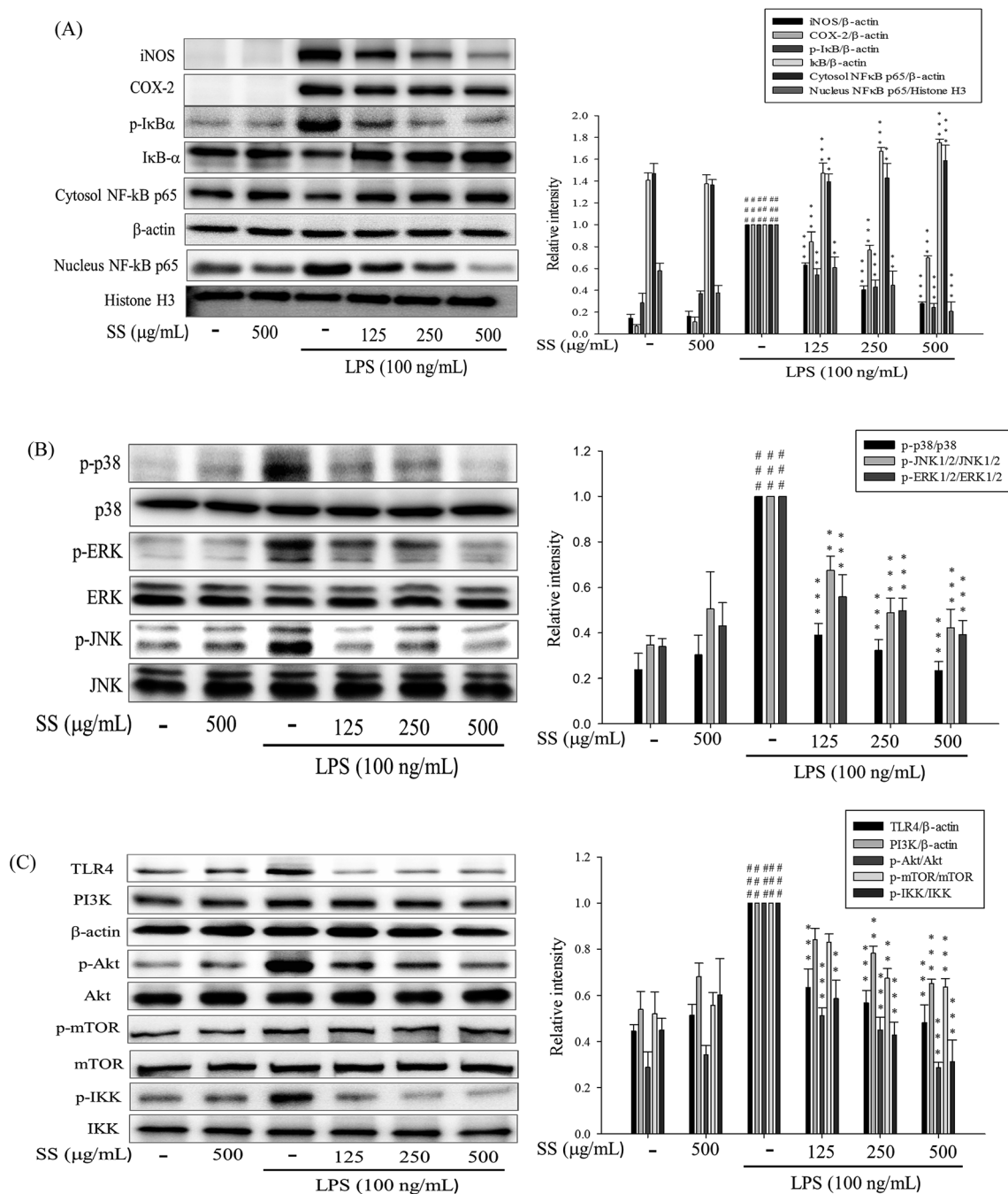
Fig. 2 Effects of SS on iNOs, COX-2, IκB-α, and NF-κB protein expression in RAW 264.7 cells. (A) MAPK phosphorylation (B) and TLR4/PI3K/Akt/mTOR/IKK protein expression (C) in LPS-induced RAW264.7 cells. Cells were incubated with or without LPS (100 ng mL^{-1}) in the presence of various concentrations (125, 250 and 500 μg mL^{-1}) of SS for 24 h. The data were presented as mean ± SD for the three different experiments performed in triplicate. ###$p < 0.001$ compared with sample of control-alone group (one-way ANOVA followed by Scheffe's multiple range tests). **$p < 0.01$, and ***$p < 0.001$ were compared with LPS-alone group.

3.6. Effect of SS on BALF cytokine levels and iNOS, COX-2 protein expressions in LPS-induced ALI mice

In the body, excessive concentrations of NO and pro-inflammatory cytokines play an important role in the pathogenesis of LPS-induced ALI. As shown in Fig. 6, compared with the control group, the LPS-induced group showed a significant increase in the concentrations of tumor necrosis factor-alpha (TNF-α), interleukin-1 beta (IL-1β),

interleukin-6 (IL-6), and NO in bronchoalveolar lavage fluid. Compared with the LPS group, the SS-administered group exhibited a significant reduction in concentrations of TNF-α, IL-1β, IL-6, and NO in bronchoalveolar lavage fluid. Furthermore, as shown in Fig. 6, there was a significant increase in the concentration of interleukin-10 (IL-10) in bronchoalveolar lavage fluid in the SS group as compared with the results observed for the LPS group.
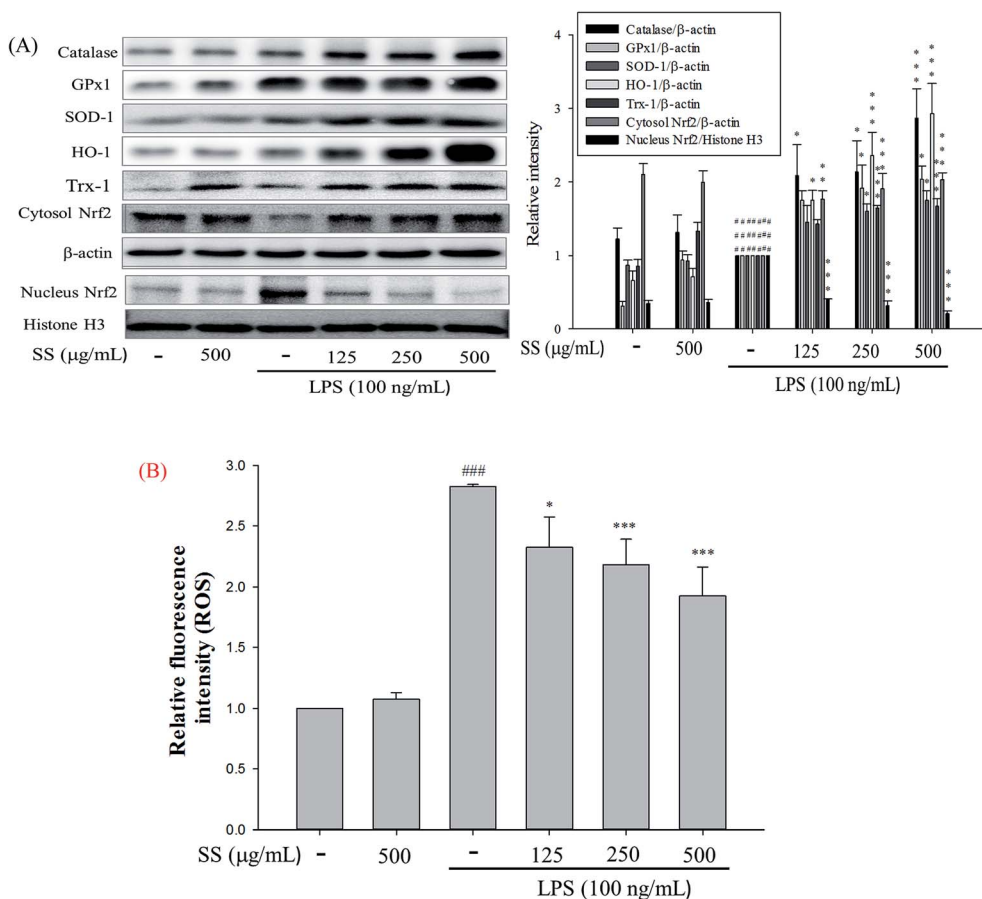
Fig. 3 Effects of SS on antioxidative enzymes, HO-1/Nrf2 protein expression (A) and ROS production (B) in LPS-induced RAW264.7 cells. Cells were incubated with or without LPS (100 ng mL^{-1}) in the presence of various concentrations (125, 250 and 500 μg mL^{-1}) of SS for 24 h. Then 10 μM DCFH-DA was added and incubated for 30 min at 37 °C. DCF fluorescence by ROS was measured by Synergy HT Microplate Reader (BioTek Instruments). The data were presented as mean ± SD for the three different experiments performed in triplicate. ###$p < 0.001$ were compared with sample of control group (one-way ANOVA followed by Scheffe's multiple range tests). *$p < 0.05$, **$p < 0.01$, and ***$p < 0.001$ were compared with LPS-alone group.
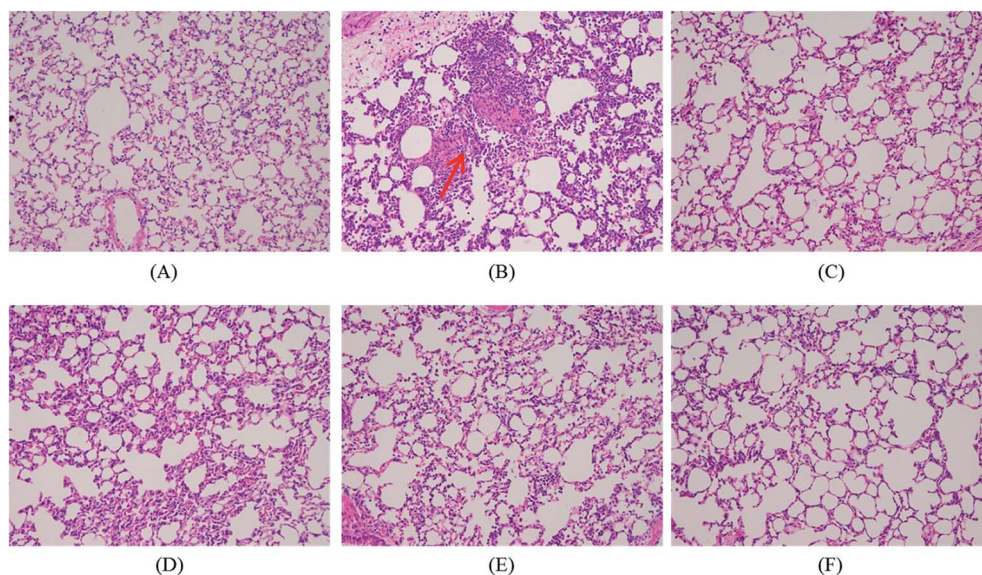

Fig. 4 SS attenuated pulmonary inflammation *in vivo*. Six hours after LPS injection with or without SS pretreatments, mice were exsanguinated and their left lower lungs were fixed. Then, tissue sections were stained with hematoxylin and eosin (H&E). The figure demonstrates a representative view (×400) from each group; each bar represents the mean ± SD of 6 mice. (A) Control; (B) LPS; (C) LPS + Dex; (D) LPS + SS-L; (E) LPS + SS-M; (F) LPS + SS-H. The infiltrating neutrophils were more abundant in (B) LPS group as shown by arrows.
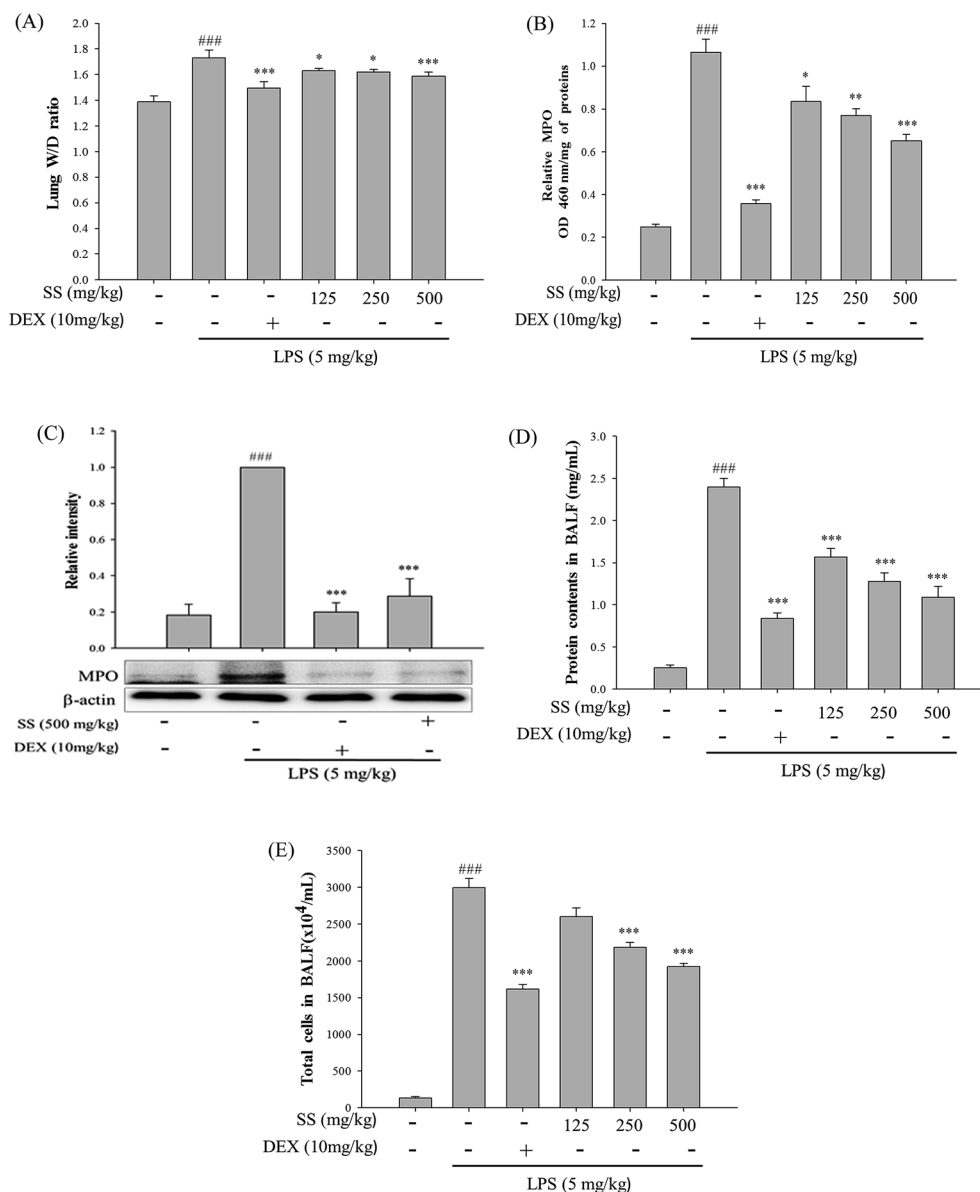
Fig. 5 SS improved pulmonary edema (A), myeloperoxidase (MPO) activity (B), MPO protein level (C) *in vivo* and reduced cellular counts (D) and total protein (E) in BALF. Six hours after LPS injection with or without SS pretreatments, mice were sacrificed and their lungs were lavaged. The right lower lungs were used to assess wet to dry (W/D) ratio of lung. Cells in the BALF were collected and cytospin preparations were made. Total cells and total proteins in BALF were analyzed. Data represents mean ± SD of 6 mice. ###$p < 0.001$ were compared with sample of control group (one-way ANOVA followed by Scheffe's multiple range tests). *$p < 0.05$, **$p < 0.01$, and ***$p < 0.001$, were compared with LPS-alone group.

The protein expression of iNOS and COX-2 was analyzed using western blot. As shown in Fig. 7, iNOS and COX-2 expression significantly increased in the LPS group as compared with the values reported for the control group whereas in the SS-administered group, there was a significant reduction in iNOS and COX-2 protein expression levels in lung tissue, as compared with levels in the LPS group.

3.7. Effects of SS on NF-κB and MAPK activation in LPS induced ALI mice

In mice with ALI, after LPS induction, the NF-κB and MAPK pathways were activated. As shown in Fig. 7, in the LPS-induced

group, the expression levels of NF-κB p65 and IκBα in cytoplasm decreased, while p-IκBα expression in cytoplasm increased, showing that LPS induction activated NF-κB p65 to enter the cell nucleus. In the SS-administered group, the expression levels of NF-κB p65 and IκBα in cytoplasm increased, and the expression of p-IκBα in cytoplasm decreased, indicating that SS can reduce NF-κB p65 entry into the cell nucleus, a significant change as compared with the LPS group. As shown in Fig. 7, LPS-alone group markedly increased the translocation of NF-κB to the nucleus. However, treatment of SS (500 mg kg^{-1}) significantly reduced the nuclear translocation of NF-κB. In addition, as compared with the LPS group, the SS-administered group had
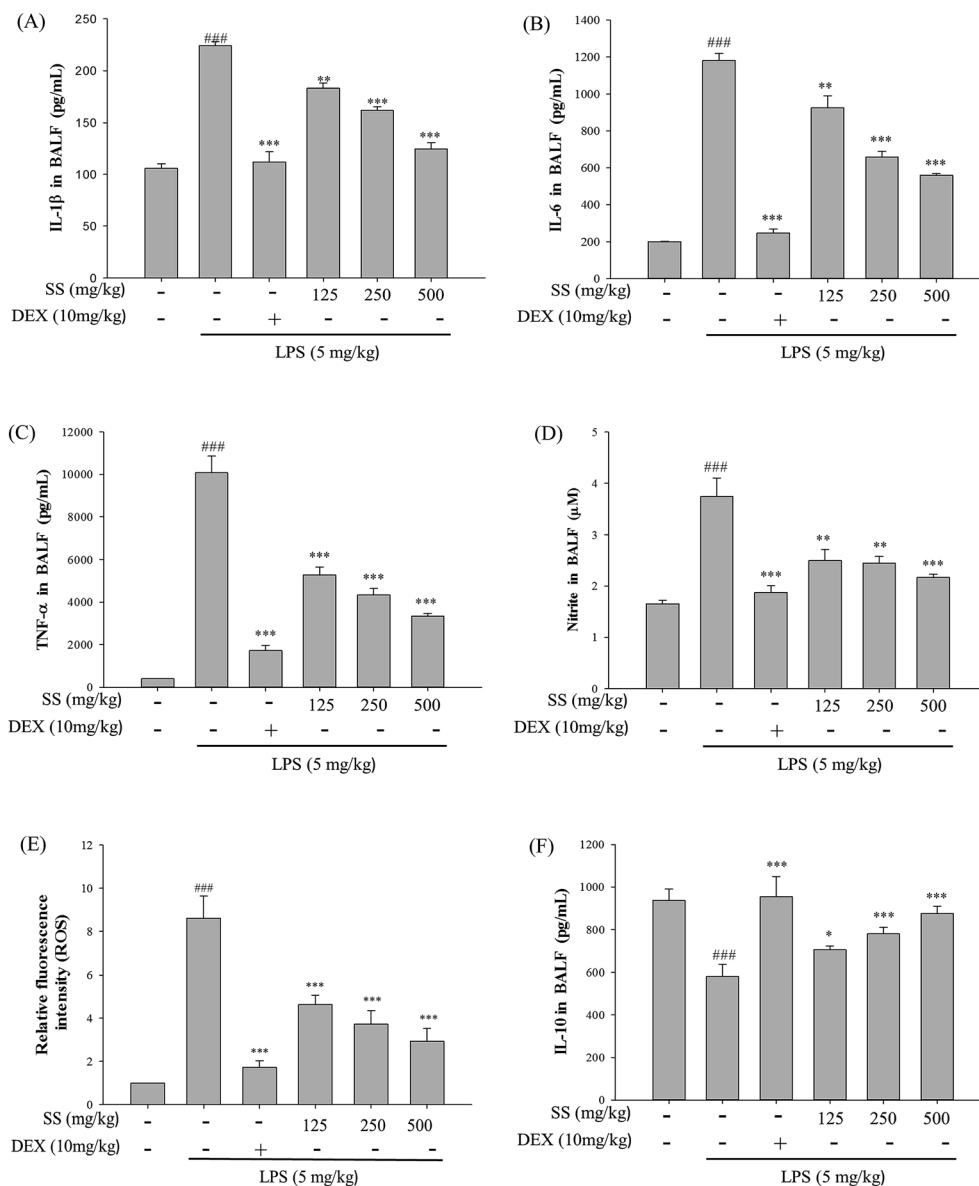
Fig. 6 SS down regulated TNF-α (A), IL-6 (B), IL-1β (C), NO (D), NO (E) and increased IL-10 (F) in BALF. Six hours after LPS injection with or without SS pre-treatments, mice were sacrificed, their lungs were lavaged and the BALF were collected. TNF-α, IL-6, IL-1β, NO and IL-10 were detected by ELISA. Then 10 μM DCFH-DA was added and incubated for 30 min at 37 °C. DCF fluorescence by ROS was measured by Synergy HT Microplate Reader (BioTek Instruments). Data represents mean ± SD of 6 mice. ###$p < 0.001$ were compared with sample of control group (one-way ANOVA followed by Scheffe's multiple range tests). *$p < 0.05$, **$p < 0.01$, and ***$p < 0.001$, were compared with LPS-alone group.

a significant reduction in ERK 1/2, JNK 1/2, and p38 phosphorylation in lung tissue, as shown in Fig. 7.

3.8. Effect of SS on TLR4/PI3K/Akt/mTOR/IKKβ pathway activation in LPS induced ALI mice

Furthermore, this study analyzed the expression levels of proteins related to the TLR4/phosphoinositide 3-kinase (PI3K)/Akt/mTOR/IκB kinase beta (IKKβ) signaling pathway. As shown in Fig. 8, TLR4 and PI3K protein expression was significantly induced, and Akt, mTOR and IKKβ protein phosphorylation increased in the LPS-induced group as compared with that reported for the control group. Compared with the LPS group,

the SS-administered group showed a significant reduction in the activity of the TLR4/PI3K/Akt/mTOR/IKKβ signaling pathway.

3.9. Effects of SS on LPS-induced antioxidative enzymes and HO-1, Trx-1/Nrf2 protein expressions in ALI mice

As shown in Fig. 8, compared with the LPS group, the group administered LPS alone showed a significant reduction in lung tissue expression levels of GPX, SOD, CAT, Trx-1, and Nrf2 proteins in the cytoplasm; however, the significant increase in lung tissue expression levels of HO-1 and Nrf2 expression in the nucleus. In addition, in the SS-administered group, the
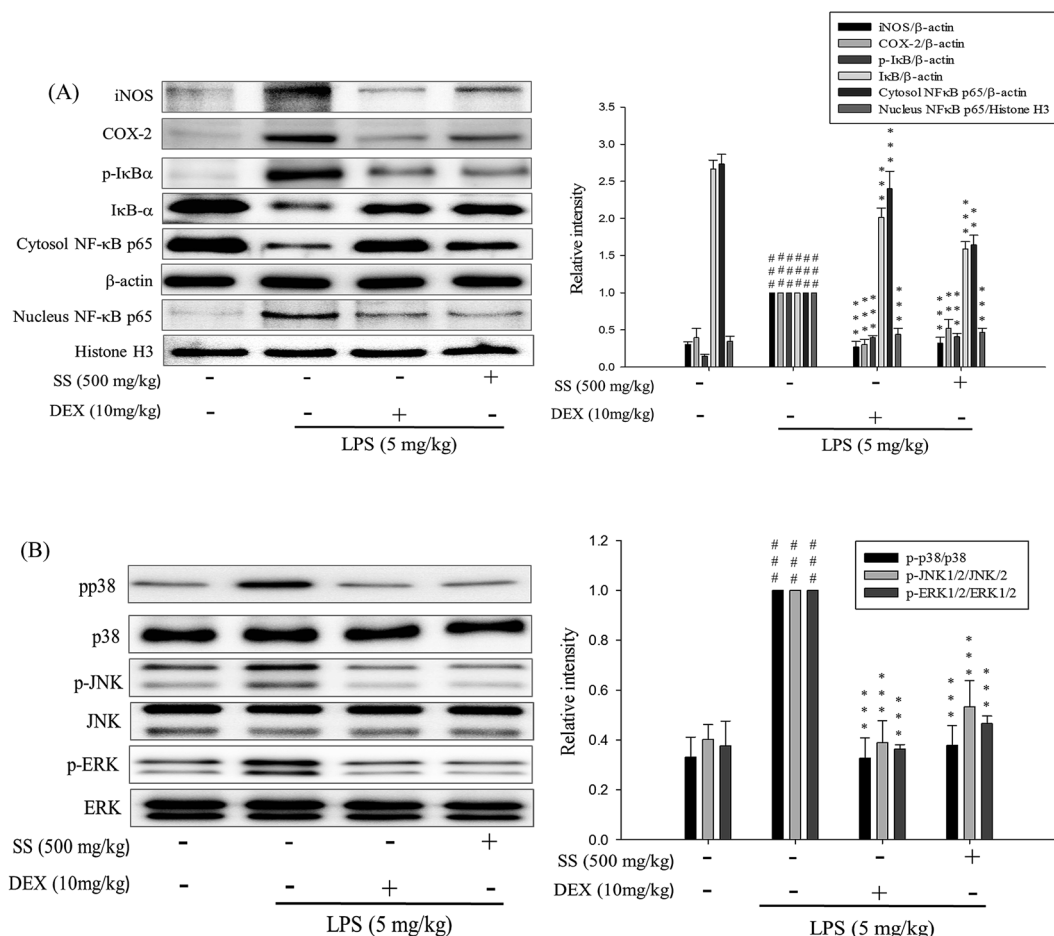
Fig. 7 Effects of SS on LPS-induced iNOs, COX-2, IκB-α, and NF-κB protein expression in lung (A), MAPK phosphorylation (B) expression in ALI mice. Mice were pretreated with different concentrations of SS for 1 h and stimulated with LPS. The Western blotting by using an antibody specific were used for the detection of iNOs, COX-2, IκB-α phosphorylated, NF-κB nuclear and cytosol, and total forms of three MAPK molecules, ERK, p38, and JNK. Data represents mean ± SD of 6 mice. ###$p < 0.001$ were compared with sample of control group (one-way ANOVA followed by Scheffe's multiple range tests). **$p < 0.01$, and ***$p < 0.001$, were compared with LPS-alone group.

expression of GPX, SOD, CAT, Trx-1, and cytoplasm of Nrf2 in lung tissue significantly increased as compared with that reported for the LPS group.

3.10.   Blocking TLR4 with TAK-242 synergistically increases the anti-inflammatory potential of SS in RAW 264.7 macrophages

To confirm involvement of the TLR4 signaling pathway in the SS-mediated anti-inflammatory potential, we selected TAK-242 (100 ng mL^{-1}) inhibit agent, which blocks TLR4-mediated signaling. As shown in Fig. 9, we found that SS and TAK-242 co-treatment synergistically inhibited LPS-induced production of NO and ROS as well as iNOS, COX-2 and NF-κB p65 expression. Furthermore, the effects of LPS-enhanced TNF-α and IL-1β release were successfully inhibited by blocking TLR4 signaling with TAK-242, and co-treatment of SS with TAK-242 almost completely inhibited the production of those pro-inflammatory cytokines to background levels similar to that in the untreated control (Fig. 9).

3.11.   Blocking TLR4 with TAK-242 synergistically increases the anti-inflammatory potential of SS in ALI mice

In mice with ALI, to determine whether TAK-242 could inhibit TLR4-mediated signaling pathways or not, we analyze TLR4 pathway related protein expression in LPS-exposed mice treatment with TAK-242 (3.0 mg kg^{-1}).

As shown in Fig. 10, the effects of LPS-induction TNF-α, IL-1β, IL-6 release were successfully inhibited by blocking TLR4 signaling with TAK-242, and co-treatment of SS with TAK-242 almost completely inhibited the production of those pro-inflammatory cytokines compared with that reported for the untreated control group. However, we found that SS and TAK-242 co-treatment synergistically inhibited LPS-induced production of NO as well as iNOS, COX-2 and NF-κB p65 expression. Furthermore, the administration of 3.0 mg kg^{-1} of TAK-242, and co-treatment of SS with TAK-242 almost markedly reduced the cell numbers, protein concentrations and MPO level in the BALF, suggesting that TAK-242 and SS might inhibit the degranulation of neutrophils (Fig. 10).
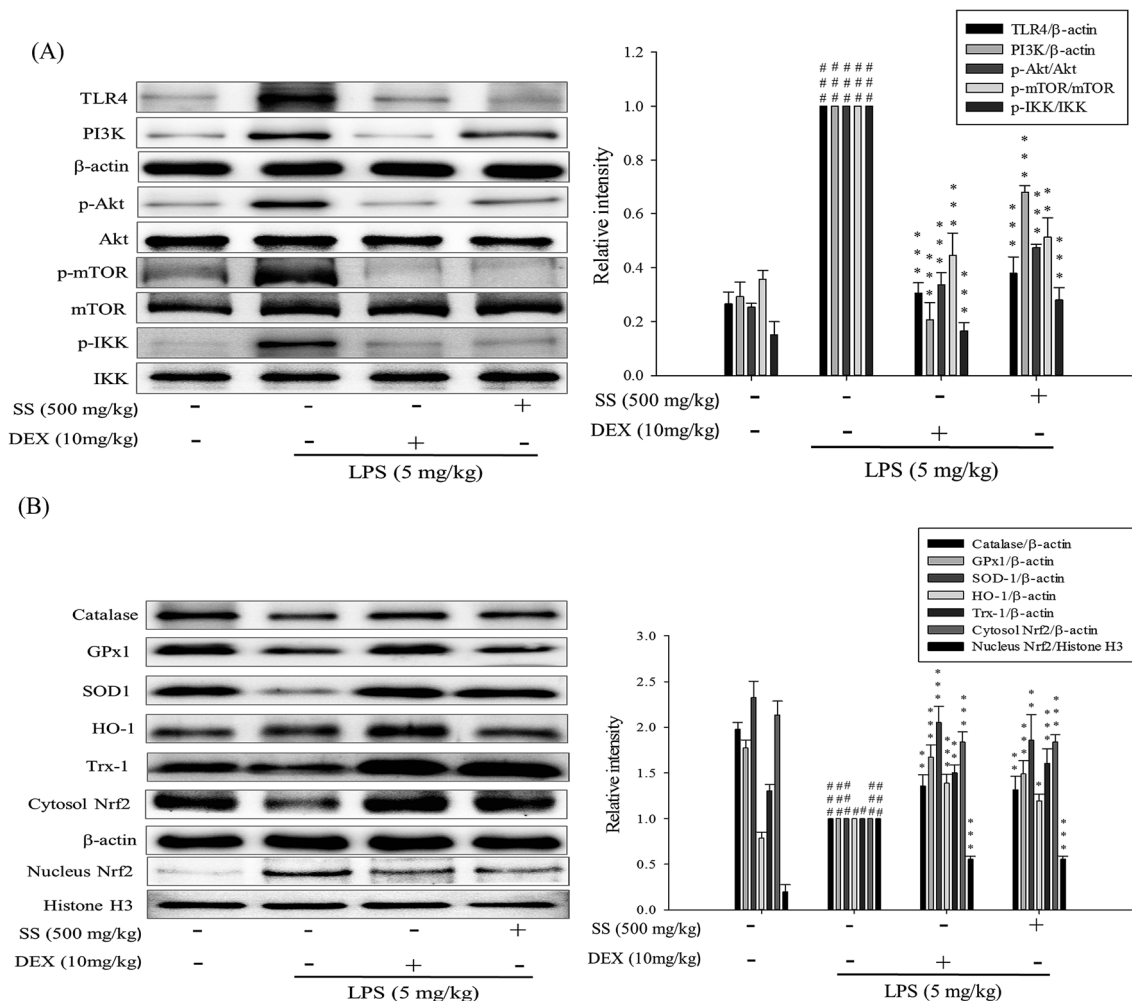
(A)

(B)
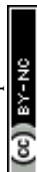
Fig. 8   Effects of SS on LPS-induced TLR4, PI3K, AKT, mTOR, and IKK protein expression and anti-oxidative enzymes, HO-1/Nrf2 protein expression in lung in ALI mice. Mice were pretreated with different concentrations of SS for 1 h and stimulated with LPS. The Western blotting by using an antibody specific were used for the detection of TLR4, PI3K, AKT, mTOR, and IKK protein expression. The Western blotting by using an antibody specific were used for the detection of HO-1/Nrf2, total forms of antioxidative enzymes, catalase, GPx1, and SOD-1Data represents mean $\pm$ SD of 6 mice. #$p < 0.05$, ###$p < 0.001$ were compared with sample of control group (one-way ANOVA followed by Scheffe's multiple range tests). **$p < 0.01$, and ***$p < 0.001$, were compared with LPS-alone group.

3.12.   HPLC profile of SS

The major components of SS were analyzed by HPLC (Fig. 10A). As compared with standard reference compounds, four compounds were identified and determined: (1) protocatechuic acid: (2) protocatechualdehyde; (3) caffeic acid; (4) DBL (3,4-dihydroxybenzalacetone).

4.   Discussion

The local protective response to tissue damage or microbial invasion is inflammation; it leads to capillary dilation, increased permeability, and leukocyte migration to the inflamed area, wherein leukocytes phagocytose or dilute pathogens.[21–23] However, an excessive or continuous inflammatory response is closely related to the development of numerous diseases, such as acute lung injury (ALI), asthma, inflammatory bowel disease, sepsis, or cancer.[24–26] In the process of

development of these diseases, the inflammatory response plays a critical role. Previous studies have found that at the site of inflammation, macrophages release large amounts of proinflammatory factors. If the production of proinflammatory substances can be inhibited, the inflammatory response can be alleviated, leading to the treatment of the disease.[27,28]

According to the results of cell experiments performed in this study, at concentrations that do not affect murine macrophage cell viability, SS can significantly regulate not only the expression of factors related to the inflammatory response but also the production of proinflammatory substances. SS administration can also improve the inflammatory nature of macrophages by inhibiting the activation of the NF-κB signaling pathway and MAPK phosphorylation.

In addition, many studies have indicated that inflammation of the lungs owing to infection is mostly caused by the release of endotoxins by Gram-negative bacteria, which are an important
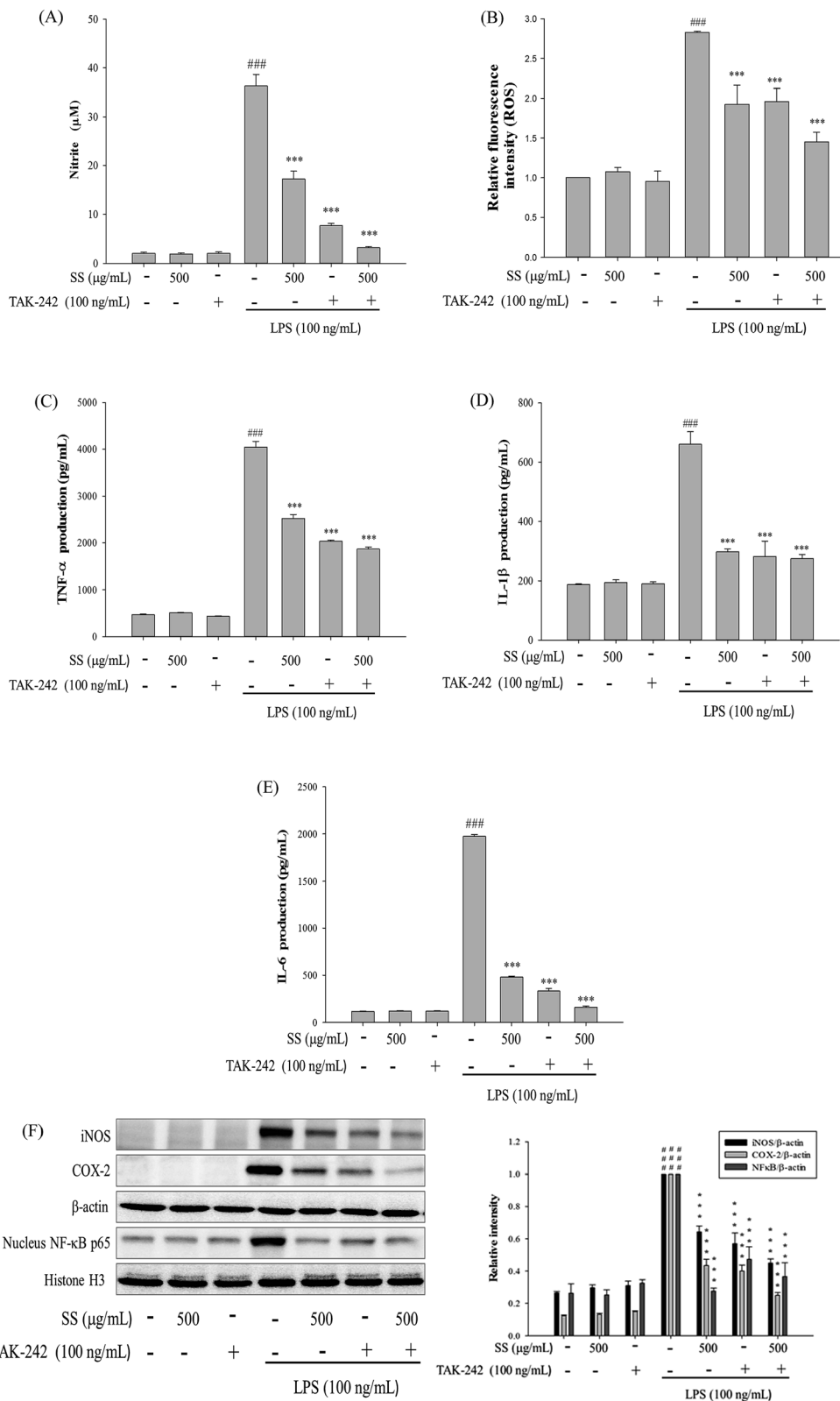
Fig. 9 SS and TAK-242 inhibited lipopolysaccharide (LPS)-induced cell inflammation in RAW 264.7 cells. NO (A), ROS (B), TNF-α (C), IL-1β (D), and IL-6 (E) production in LPS-stimulated RAW264.7 cells. Effects of SS and TAK-242 on iNOs, COX-2, and NF-κB protein expression in RAW 264.7 cells (F). Cells were incubated with or without LPS (100 ng mL^{-1}) in TAK-242 at 100 ng mL^{-1} or SS at 500 μg mL^{-1} for 24 h. The data were presented as mean ± SD for the three different experiments performed in triplicate. ###$p < 0.001$ compared with sample of control-alone group (one-way ANOVA followed by Scheffe's multiple range tests). ***$p < 0.001$ were compared with LPS-alone group.
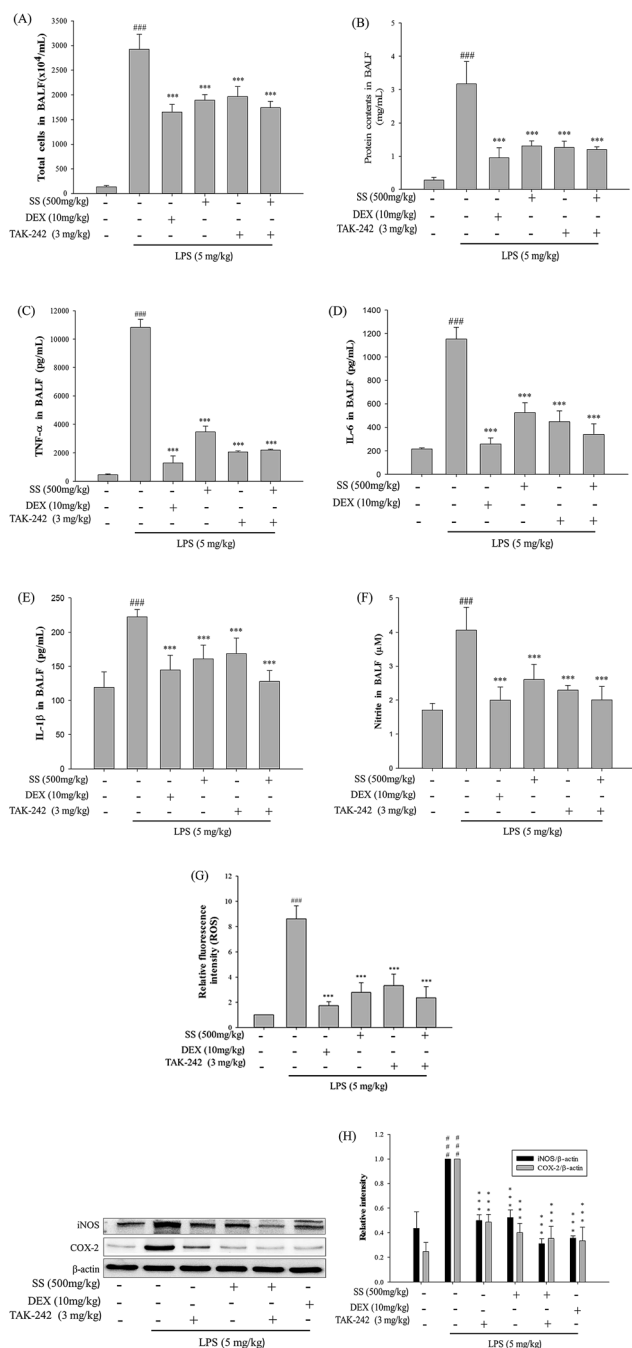
Fig. 10 SS and TAK-242 reduced cellular counts (A), total protein (B), TNF-α (C), IL-6 (D), IL-1β (E), NO (F), ROS (G), in BALF and down regulated iNOs and COX-2 protein expression (H) in lung. Mice were pretreated with different concentrations of SS and TAK-242 for 1 h and stimulated with LPS. The Western blotting by using an antibody specific were used for the detection of iNOs, COX-2, NF-κB nuclear and cytosol. Data represents mean ± SD of 6 mice. Six hours after LPS injection with or without SS and TAK-242 pre-treatments, mice were sacrificed, their lungs were lavaged and the BALF were collected. TNF-α, IL-6, IL-1β, NO and IL-10 were detected by ELISA. Data represents mean ± SD of 6 mice. ###$p < 0.001$ compared with sample of control group (one-way ANOVA followed by Scheffe's multiple range tests). ***$p < 0.001$, were compared with LPS-alone group.

pathogenic factor.[25] Therefore, ALI animal models induced by intratracheal instillation of endotoxins are often adopted to investigate the pathogenic mechanism underlying ALI and its effective treatments.

These models are established by intratracheal instillation of LPS in mice, which induces changes in the pulmonary microvascular epithelium and permeability of epithelial cells that lead to pulmonary edema. Meanwhile, this instillation drives large numbers of leukocytes to gather in the inflamed interstitial tissues. Furthermore, large amounts of neutrophils, as well as significantly increased MPO activity can be found in microvessels in lung biopsy tissue sections.[26] This study reported similar findings, indicating that neutrophils play an important role in the process of inflammation caused by endotoxins. This is mainly because activated neutrophils can release large amounts of free radicals and proteases that promote pulmonary edema and microvascular permeability.

In this study, 6 hours after intratracheal instillation of LPS, a significant increase in wet/dry lung tissue weight ratios and protein contents of bronchoalveolar lavage fluid was observed. This shows that since the cytoskeleton may contract when epithelial cells are damaged, changes occur in the space within epithelial cells, leading to an increase in vascular permeability, and this subsequent increase in vascular permeability allows moisture in the blood to enter the interstitial space in the lungs more easily, resulting in formation of pulmonary edema.[26–29] In cases of more severe damage to epithelial cells, the accompanying changes in vascular permeability allow large protein molecules to enter the interstitial space in the lungs, causing an increase in the concentration of proteins in bronchial washings.[25]

Administration of 125, 250, and 500 mg kg⁻¹ SS over 5 consecutive days following LPS induction decreased the wet/dry lung tissue weight ratio, as well as the total cell numbers and protein concentrations in bronchial washings. These results suggests that the reduction may be due to the ability of SS to reduce damage to pulmonary microvessels and alveolar cells by reducing the release of proinflammatory substances and free radicals, thereby changing the permeability of pulmonary microvessels. Additionally, prior administration of SS can reduce not only the accumulation of leukocytes in bronchial washings but also MPO activity in lung tissues.

Further observation of lung tissue sections showed that when murine lung tissue was damaged, neutrophil accumulation and injury decreased in the lung tissues of the SS-administered group. Therefore, it was speculated that sanghuang extract can reduce the production of proinflammatory substances by reducing the infiltration of neutrophils, thereby improving the damage caused to alveolar epithelial cells and pulmonary microvascular endothelial cells.

Furthermore, stimulation of lung tissues by endotoxins promoted the activity of neutrophils and macrophages in pulmonary tissues and triggered the release of a large number of proinflammatory cytokines, such as TNF-α, IL-1β, and IL-6 as well as free radicals that can continue the inflammatory process, leading to more serious tissue inflammation and even apoptosis.[29–32] Based on the results of this study, a significant
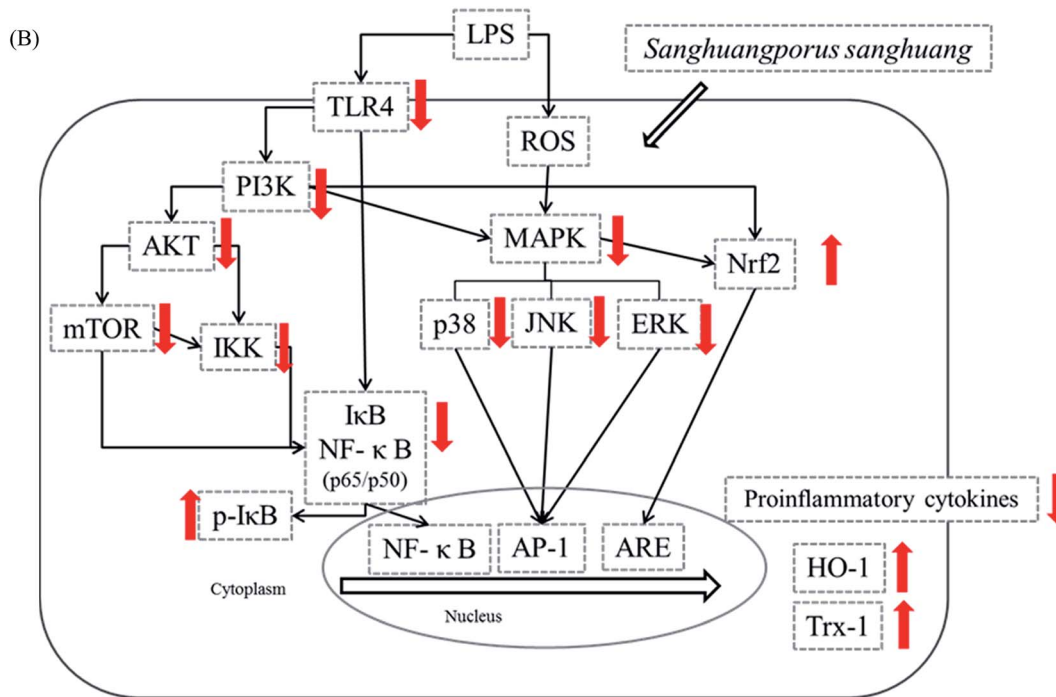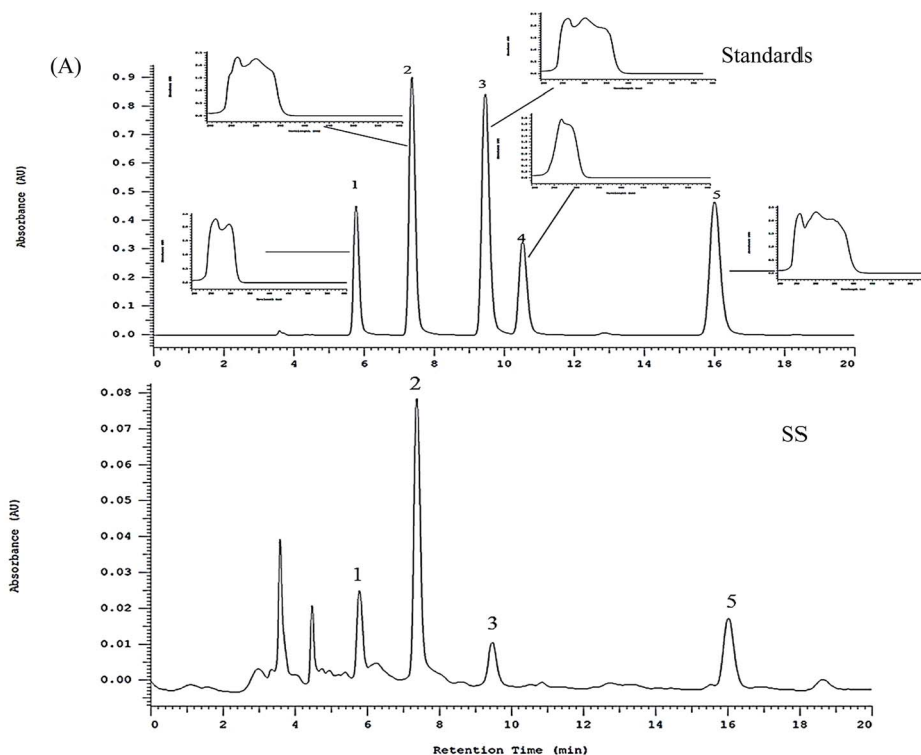
Fig. 11 HPLC-DAD profile of SS (A) and schemes of the mechanism for the protective effect of is on LPS-induced inflammation (B). HPLC chromatogram of the polyphenol standards at 280 nm. Peaks: (1) protocatechuic acid (5.76 min); (2) protocatechualdehyde (7.37 min); (3) caffeic acid (9.46 min); (4) syringic acid (10.53 min); (5) DBL (16.0 min). Representative chromatograms of SS were shown respectively. (1) Protocatechuic acid; (2) protocatechualdehyde; (3) caffeic acid; (4) DBL (3,4-dihydroxybenzalacetone).

increase in TNF-α, IL-1β, and IL-6 concentrations in bronchoalveolar lavage fluid was observed after LPS induction. This shows that when tissues are subjected to foreign infection, inflammatory cells are driven to release large amounts of inflammatory substances, which indirectly activate the immune system, leading to an inflammatory response as a means to clear the foreign infectious substances.[32,33]

In the present study, prior administration of SS improved damage to the lung tissue by reducing the production of TNF-α, IL-1β, and IL-6 in bronchoalveolar lavage fluid caused by LPS

induction, and increasing the concentration of IL-10 and cytokine synthesis inhibitory factor.

As shown in previous studies, NO is released in large amounts in the LPS-induced ALI model. Furthermore, when the inflammatory response is stimulated, neutrophils, macrophages, endothelial and epithelial cells activate iNOS and produce large amounts of NO, which further attacks pulmonary microvascular endothelial cells, causing damage to lung tissues.[31,32] The results of this study show that prior administration of SS can improve damage to lung tissues that is caused by LPS-induced ALI, by reducing the expression of iNOS and COX-2 in the lung tissues.

When LPS binds to TLR4 expressed by cells, the physiological role of cells is altered owing to activation of signaling pathways related to either cell survival or the inflammatory response. Previous studies have shown that LPS causes phosphorylation of Akt through PI3K, and phosphorylated Akt promotes activation of the NF-κB and MAPK downstream signaling pathways through IKK, which regulates the release of proinflammatory cytokines by the respiratory epithelium and maintains cell viability.[9,27,29–34] Recent studies have implicated mTOR in the regulation of cell survival and immune responses. mTOR is downstream of PI3K/Akt during signal transduction. Akt can phosphorylate mTOR, which interacts with IKK, leading to NF-κB activation. mTOR plays an important role in LPS-induced inflammatory responses. Inhibition of mTOR can reduce NF-κB phosphorylation in neutrophil leukocytes and pro-inflammatory cytokine expression.[8,10,34–36] According to the results of this study, prior administration of SS can reduce activation of the signaling pathways triggered by LPS induction by regulating TLR4/PI3K/Akt/mTOR and IKK protein expression levels. This inhibits NF-κB from actively entering the nucleus and reduces phosphorylation of the MAPK pathway, thus not only reducing the release of proinflammatory cytokines and inflammatory substances, but also improving damage to lung tissues.

TAK-242, is a selective TLR4 signal transduction inhibitor. According to the relevant research has been shown TAK-242 can reduce production of multiple inflammatory mediators such as nitric oxide (NO), tumor necrosis factor (TNF)-α, interleukin (IL)-1, IL-6.[37–39] Moreover, TAK-242 also effectively attenuated the neutrophil activation and accumulation in the lungs, as well as inhibited the DNA binding activation of NF-kB induced by LPS challenge.[40] Therefore, TAK-242 may be a potential inhibitor of adhesion molecules and inflammatory mediators. In this study, we selected TAK-242 inhibitors as evidence that SS could regulate LPS-induced TLR4 pathway-related protein expression *in vitro* and *in vivo*.[41–46]

In addition, combined pretreatment of SS with TAK-242, synergistically attenuated the release of NO, as well as expression of iNOS, COX-2 and NF-κB p65 protein, *in vitro* and *in vivo*. In accordance with these results, co-treatment also reduced the production and expression of ROS, TNF-α, IL-6, IL-1β compared to those in the SS or TAK-242 alone treated groups in LPS-treated RAW 264.7 macrophages. However, we also found the same results in LPS-induced acute lung injury in mice. Additionally, prior administration of SS and TKA-242 co-treatment

can reduce not only the accumulation of leukocytes in bronchial washings but also MPO activity in lung tissues.

According to our results show that SS may inhibit the initiation of intracellular inflammatory signaling cascades by attenuating the binding of LPS to TLR4 on macrophages, which is a pivotal upstream signal for NF-κB p65 activation. Therefore, the antagonistic function of SS against TLR4 may be responsible for the anti-inflammatory effects of SS in LPS-stimulated RAW 264.7 macrophages or LPS-induced ALI mice.

In the LPS-induced ALI mouse model, large amounts of ROS were produced, mainly because after neutrophils were activated by LPS, large amounts of surplus oxides, hydrogen peroxide, and reactive oxygen species were released as a means to kill or remove foreign pathogens. However, if excess ROS is produced, there is no way for the body's antioxidant system to remove them in a timely manner, causing the inflamed tissue to be aggravated and the situation to be exacerbated.[10,11,13,47] Based on the results of this study, prior administration of SS can reduce the production of ROS that is caused by LPS-induced ALI in tissues. It was speculated that the possible signaling pathway might involve the regulation of levels of protein phosphorylation related to the MAPK signaling pathway, and collaboration with the body's antioxidant enzymes, such as SOD, CAT, GPX, which remove large amounts of ROS from the body, thus alleviating damage caused to tissues.

In addition, HO-1 expression can regulate the cellular inflammatory response by, such as, regulating the cellular inflammatory response induced by TNF-α and reducing cell-induced cytokine production.[48] Presently, most studies also suggest that when cells are stimulated by external factors, the cellular protective mechanism is initiated and HO-1 expression is induced to resist the attacks by foreign bodies.

The lung is the organ with the highest oxygen content and is susceptible to damage by active oxygen. Redox equilibrium in cells is essential for sustaining the physiological functions of the lung, as well as regulating intracellular and intercellular chemical reactions and signal transductions. Thioredoxin-1 (Trx-1), a significant redox molecule, plays an important role in antioxidative activities and promoting interconversions between protein disulfide bonds and thiols.[49] In recent decades, the effects of Trx-1 in lung diseases have been increasingly recognized. Trx-1 is extensively expressed in various lung cells and regulates intracellular oxidative stress and inflammatory responses.[50] Trx-1 can be regarded as an anti-inflammatory agent and antioxidant. Furthermore, Nrf2 is overexpressed in detoxifying organs, such as the liver and kidneys, as well as organs that are exposed to the external environment, such as the skin, lungs, and intestinal tract. However, when cells are subjected to a variety of stimuli, the Nrf2 protein binds to the antioxidant response agent (ARE), and participates in the regulation of expression of related antioxidant enzymes, such as HO-1 and Trx-1, to remove oxidative stress.[22,26,47,50] Based on the results of this study, SS contains many polyphenolic compounds, which bear OH groups in their structure and exhibit free radical scavenging ability. Thus, it plays a synergistic role with antioxidant enzymes in eliminating LPS-induced ROS in tissues and therefore, alleviating lung tissue injury.

A summary of the results presented in this paper suggests that in LPS-induced ALI, prior administration of SS can trigger related protection mechanism of LPS-induced ALI, as shown in Fig. 11B.

5. Conclusions

In conclusion, according to the results of this study, sanghuang has a moderate anti-inflammatory activity. Both *in vitro* and *in vivo* tests showed that sanghuang can regulate TLR4/PI3K/Akt/mTOR and IKK protein expression levels, inhibit NF-κB from actively entering the nucleus, and reduce phosphorylation of the MAPK pathway, thus reducing the cellular release of proinflammatory cytokines and inflammatory substances, and alleviating damage to lung tissues. In addition, SS can also co-antioxidant enzymes (HO-1 and Trx-1) inhibit cell inflammation, and removing large amounts of ROS to improve damage to lung tissues. Sanghuang has considerable potential in the treatment or prevention of inflammatory diseases, such as ALI.

Author contributions

Wang-Ching Lin conducted majority of the experiments and prepared the first draft of the manuscript. Guan-Jhong Huang and Wan-Rong Lin conducted the ALI experiment and the interpreted the results. Shyh-Shyun Huang, Jeng-Shyan Deng and Guan-Jhong Huang participated in data interpretation and helped to draft the manuscript. Hui-Yi Lin supervised the research work and proofread the manuscript. The fruiting body of *S. sanghuang* grown on mulberry tree used in this study was provided by Chin-Chu Chen and its species was confirmed by Sheng-Hua Wu.

Conflicts of interest

The authors declare no conflict of interest.

Acknowledgements

References

1 Y. Liu, H. Wu, Y. C. Nie, J. L. Chen, W. W. Su and P. B. Li, Naringin attenuates acute lung injury in LPS-treated mice by inhibiting NF-κB pathway, *Int. Immunopharmacol.*, 2011, **11**, 606–1612.

2 N. Niu, B. Li, Y. Hu, X. Li, J. Li and H. Zhang, Protective effects of scoparone against lipopolysaccharide-induced acute lung injury, *Int. Immunopharmacol.*, 2014, **23**, 127–133.

3 K. L. Huang, C. S. Chen, C. W. Hsu, M. H. Li, H. Chang, S. H. Tsai and S. J. Chu, Therapeutic effects of baicalin on lipopolysaccharide-induced acute lung injury in rats, *Am. J. Chin. Med.*, 2008, **36**, 301–311.

4 C. L. Tsai, Y. C. Lin, H. M. Wang and T. C. Chou, Baicalein, an active component of *Scutellaria baicalensis*, protects against lipopolysaccharide-induced acute lung injury in rats, *J. Ethnopharmacol.*, 2014, **153**, 197–206.

5 N. Yang, C. Li, G. Tian, M. Zhu, W. Bu, J. Chen, X. Hou, L. Di, X. Jia, Z. Dong and L. Feng, Organic acid component from *Taraxacum mongolicum Hand.-Mazz* alleviates inflammatory injury in lipopolysaccharide-induced acute tracheobronchitis of ICR mice through TLR4/NF-κB signaling pathway, *Int. Immunopharmacol.*, 2016, **34**, 92–100.

6 C. H. Huang, M. L. Yang, C. H. Tsai, Y. C. Li, Y. J. Lin and Y. H. Kuan, *Ginkgo biloba* leaves extract (EGb-761) attenuates lipopolysaccharide-induced acute lung injury *via* inhibition of oxidative stress and NF-κB-dependent matrix metalloproteinase-9 pathway, *Phytomedicine*, 2013, **20**, 303–309.

7 P. J. Yu, J. R. Li, Z. G. Zhu, H. Y. Kong, H. Jin, J. Y. Zhang, Y. X. Tian, Z. H. Li, X. Y. Wu, J. J. Zhang and S. G. Wu, Praeruptorin D and E attenuate lipopolysaccharide/hydrochloric acid induced acute lung injury in mice, *Eur. J. Pharmacol.*, 2013, **710**, 39–48.

8 Y. Wang, Y. Liu, X. Y. Zhang, L. H. Xu, D. Y. Ouyang, K. P. Liu, H. Pan, J. He and X. H. He, Ginsenoside Rg1 regulates innate immune responses in macrophages through differentially modulating the NF-κB and PI3K/Akt/mTOR pathways, *Int. Immunopharmacol.*, 2014, **23**(1), 77–84.

9 J. H. Kim, Y. Y. Choo, N. Tae, B. S. Min and J. H. Lee, The anti-inflammatory effect of 3-deoxysappanchalcone is mediated by inducing heme oxygenase-1 *via* activating the AKT/mTOR pathway in murine macrophages, *Int. Immunopharmacol.*, 2014, **22**(2), 420–426.

10 Y. Hu, J. Liu, Y. F. Wu, J. Lou, Y. Y. Mao, H. H. Shen and Z. H. Chen, mTOR and autophagy in regulation of acute lung injury: a review and perspective, *Microbes Infect.*, 2014, **16**(9), 27–34.

11 K. C. Li, Y. L. Ho, C. Y. Chen, W. T. Hsieh, Y. S. Chang and G. J. Huang, Lobeline improves acute lung injury *via* nuclear factor-κB-signaling pathway and oxidative stress, *Respir. Physiol. Neurobiol.*, 2016, **225**, 19–30.

12 C. H. Yeh, J. J. Yang, M. L. Yang, Y. C. Li and Y. H. Kuan, Rutin decreases lipopolysaccharide-induced acute lung injury *via* inhibition of oxidative stress and the MAPK-NF-κB pathway, *Free Radical Biol. Med.*, 2014, **69**, 249–257.

13 S. H. Wu, Y. C. Dai, T. Hattori, T. W. Yu, D. M. Wang, E. Parmasto, H. Y. Chang and S. Y. Shin, Species clarification for the medicinally valuable 'sanghuang' mushroom, *Bot. Stud.*, 2012, **53**, 135–149.

14 D. Abate and S. H. Wu, Global diversity and taxonomy of the *Inonotus linteus* complex (hymenochaetales, basidiomycota): *Sanghuangporus* gen. nov., *Tropicoporus excentrodendri* and *T. guanacastensis* gen. et spp. nov., and 17 new combinations, *Fungal Divers*, 2016, **77**, 335–347.
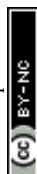
15 Y. C. Chen, H. Y. Chang, J. S. Deng, J. J. Chen, S. S. Huang, I. H. Lin, W. L. Kuo, W. Chao and G. J. Huang, Hispolon from *Phellinus linteus* induces G0/G1 cell cycle arrest and apoptosis in NB4 human leukaemia cells, *Am. J. Chin. Med.*, 2013, **41**, 1439–1457.

16 W. C. Lin, J. S. Deng, S. S. Huang, S. H. Wu, H. Y. Lin and G. J. Huang, Evaluation of antioxidant, anti-inflammatory and anti-proliferative activities of ethanol extracts from different varieties of sanghuang species, *RSC Adv.*, 2017, **7**, 7780.

17 G. J. Huang, S. S. Huang and J. S. Deng, Anti-inflammatory activities of inotilone from *Phellinus linteus* through the inhibition of MMP-9, NF-κB, and MAPK activation *in vitro* and *in vivo*, *PLoS One*, 2012, **7**, e35922.

18 W. C. Lin, J. S. Deng, S. S. Huang, S. H. Wu, C. C. Chen, W. R. Lin, H. Y. Lin and G. J. Huang, Anti-Inflammatory Activity of *Sanghuangporus sanghuang* Mycelium, *Int. J. Mol. Sci.*, 2017, **18**, 347.

19 S. H. Kim, H. S. Lee, S. Lee, J. Cho, K. Ze, J. Sung and Y. C. Kim, Mycelial culture of Phellinus linteus protectsprimary cultured rat hepatocytes against hepatotoxins, *J. Ethnopharmacol.*, 2004, **95**, 367–372.

20 P. W. Hsieh, J. B. Wu and Y. C. Wu, Chemistry and biology of *Phellinus linteus*, *Biomedicine*, 2013, 106–113.

21 P. H. Shie, S. Y. Wang, H. L. Lay and G. J. Huang, 4,7-Dimethoxy-5-methyl-1,3-benzodioxole from *Antrodia camphorata* inhibits LPS-induced inflammation *via* suppression of NF-B and induction HO-1 in RAW264.7 cells, *Int. Immunopharmacol.*, 2016, **31**, 186–194.

22 P. H. Shie, S. S. Huang, J. S. Deng and G. J. Huang, *Spiranthes sinensis* Suppresses Production of Pro-Inflammatory Mediators by Down-Regulating the NF-kB Signaling Pathway and Up-Regulating HO-1/Nrf2 Anti-Oxidant Protein, *Am. J. Chin. Med.*, 2015, **43**, 969–989.

23 S. H. Liu, T. H. Lu, C. C. Su, I. S. Lay, H. Y. Lin, K. M. Fang, T. J. Ho, K. L. Chen, Y. C. Su, W. C. Chiang, *et al.*, Lotus leaf (*Nelumbo nucifera*) and its active constituents prevent inflammatory responses in macrophages *via* JNK/NF-κB signaling pathway, *Am. J. Chin. Med.*, 2014, **42**, 869–889.

24 S. Khan, R. J. Choi, O. Shehzad, H. P. Kim, M. N. Islam, J. S. Choi and Y. S. Kim, Molecular mechanism of capillarisin-mediated inhibition of MyD88/TIRAP inflammatory signaling in *in vitro* and *in vivo* experimental models, *J. Ethnopharmacol.*, 2013, **145**, 626–637.

25 N. Bhaskaran, S. Shukla, R. Kanwal, J. K. Srivastava and S. Gupta, Induction of heme oxygenase-1 by chamomile protects murine macrophages against oxidative stress, *Life Sci.*, 2012, **90**, 1027–1033.

26 B. Li, H. J. Choi, D. S. Lee, H. Oh, Y. C. Kim, J. Y. Moon, W. H. Park, S. D. Park and J. E. Kim, *Amomum Tsao-ko* suppresses lipopolysaccharide-induced inflammatory responses in RAW264.7 macrophages *via* Nrf2-dependent heme oxygenase-1 expression, *Am. J. Chin. Med.*, 2014, **42**, 1229–1244.

27 T. Yayeh, M. Hong, Q. Jia, Y. C. Lee, H. J. Kim, E. Hyun, T. W. Kim and M. H. Rhee, Pistaciachinensis inhibits NO production and upregulates HO-1 induction *via* PI3K/Akt

pathway in LPS stimulated macrophage cells, *Am. J. Chin. Med.*, 2012, **40**, 1085–1097.

28 Y. Shi, B. Zhang, X. J. Chen, D. Q. Xu, Y. X. Wang, H. Y. Dong, S. R. Ma, R. H. Sun, Y. P. Hui and Z. C. Li, Osthole protects lipopolysaccharide-induced acute lung injury in mice by preventing down-regulation of angiotensin-converting enzyme 2, *Eur. J. Pharm. Sci.*, 2013, **48**, 819–824.

29 P. K. Fu, C. Y. Yang, T. H. Tsai and C. L. Hsieh, *Moutan cortex radices* improves lipopolysaccharide-induced acute lung injury in rats through anti-inflammation, *Phytomedicine*, 2012, **19**, 1206–1215.

30 X. Zhang, H. Huang, T. Yang, Y. Ye, J. Shan, Z. Yin and L. Luo, Chlorogenic acid protects mice against lipopolysaccharide-induced acute lung injury, *Injury*, 2010, **41**, 746–752.

31 G. J. Huang, J. S. Deng, C. C. Chen, C. J. Huang, P. J. Sung, S. S. Huang and Y. H. Kuo, Methanol extract of *Antrodia camphorata* protects against lipopolysaccharide-induced acute lung injury by suppressing NF-κB and MAPK pathways in mice, *J. Agric. Food Chem.*, 2014, **62**, 5321–5329.

32 Z. San, Y. Fu, W. Li, E. Zhou, Y. Li, X. Song, T. Wang, Y. Tian, Z. Wei, M. Yao, Y. Cao and N. Zhang, Protective effect of taraxasterol on acute lung injury induced by lipopolysaccharide in mice, *Int. Immunopharmacol.*, 2014, **19**, 342–350.

33 J. S. Deng, S. S. Huang, T. H. Lin, M. M. Lee, C. C. Kuo, P. J. Sung, W. C. Hou, G. J. Huang and Y. H. Kuo, The analgesic and anti-inflammatory bioactivities of eburicoic acid and dehydroeburicoic acid isolated from *Antrodia camphorata* on the inflammatory mediator expression in mice, *J. Agric. Food Chem.*, 2013, **61**, 5064–5071.

34 C. Ma, L. Zhu, J. Wang, H. He, X. Chang, J. Gao, W. Shumin and T. Yan, Anti-inflammatory effects of water extract of *Taraxacum mongolicum hand.-Mazz* on lipopolysaccharide-induced inflammation in acute lung injury by suppressing PI3K/Akt/mTOR signaling pathway, *J. Ethnopharmacol.*, 2015, **168**, 349–355.

35 J. A. Fielhaber, S. F. Carroll, A. B. Dydensborg, M. Shourian, A. Triantafillopoulos, S. Harel, S. N. Hussain, M. Bouchard, S. T. Qureshi and A. S. Kristof, Inhibition of mammalian target of rapamycin augments lipopolysaccharide-induced lung injury and apoptosis, *J. Immunol.*, 2012, **188**(9), 4535–4542.

36 L. Wang, Y. S. Gui, X. L. Tian, B. Q. Cai, D. T. Wang, D. Zhang, H. Zhao and K. F. Xu, Inactivation of mammalian target of rapamycin (mTOR) by rapamycin in a murine model of lipopolysaccharide-induced acute lung injury, *Chin. Med. J.*, 2011, **124**(19), 3112–3117.

37 D. Wang, K. Tao, J. Xion, S. Xu, Y. Jiang, Q. Chen and S. He, TAK-242 attenuates acute cigarette smoke-induced pulmonary inflammation in mouse *via* the TLR4/NF-kB signaling pathway, *Biochem. Biophys. Res. Commun.*, 2016, **472**, 508–515.

38 M. Ii, N. Matsunaga, K. Hazeki, K. Nakamura, K. Takashima, T. Seya, O. Hazeki, T. Kitazaki and Y. Iizawa, A novel cyclohexene derivative, ethyl (6*R*)-6-[*N*-(2-chloro-4-fluorophenyl) sulfamoyl] cyclohex-1-ene-1-carboxylate (TAK-242), selectively

inhibits toll-like receptor 4-mediated cytokine production through suppression of intracellular signaling, *Mol. Pharmacol.*, 2006, **69**(4), 1288–1295.

39 T. Sha, M. Sunamoto, T. Kitazaki, J. Sato, M. Ii and Y. Iizawa, Therapeutic effects of TAK-242, a novel selective Toll-like receptor 4 signal transduction inhibitor, in mouse endotoxin shock model, *Eur. J. Pharmacol.*, 2007, **571**, 231–239.

40 H. Seki, S. Tasaka, K. Fukunaga, Y. Shiraishi, K. Moriyama, K. Miyamoto, Y. Nakano, N. Matsunaga, K. Takashima, T. Matsumoto, M. Ii, A. Ishizaka and J. Takeda, Effect of Toll-like receptor 4 inhibitor on LPS-induced lung injury, *Inflammation Res.*, 2010, **59**(10), 837–845.

41 Y. H. Choi, G. Y. Kim and H. H. Lee, Anti-inflammatory effects of cordycepin in lipopolysaccharide-stimulated RAW 264.7 macrophages through Toll-like receptor 4-mediated suppression of mitogen-activated protein kinases and NF-κB signaling pathways, *Drug Des., Dev. Ther.*, 2014, **16**, 1941–1953.

42 H. H. Lee, M. H. Han, H. J. Hwang, G. Y. Kim, S. K. Moon, J. W. Hyun, W. J. Kim and Y. H. Choi, Diallyl trisulfide exerts anti-inflammatory effects in lipopolysaccharide-stimulated RAW 264.7 macrophages by suppressing the Toll-like receptor 4/nuclear factor-κB pathway, *Int. J. Mol. Med.*, 2015, **35**, 487–495.

43 N. Matsunaga, N. Tsuchimori, T. Matsumoto and M. Ii, TAK-242 (resatorvid), a small-molecule inhibitor of Toll-like receptor (TLR) 4 signaling, binds selectively to TLR4 and interferes with interactions between TLR4 and its adaptor molecules, *Mol. Pharmacol.*, 2011, **79**, 34–41.

44 S. A. Woller, S. B. Ravula, F. C. Tucci, G. Beaton, M. Corr, R. R. Isseroff, A. M. Soulika, M. Chigbrow, K. A. Eddinger and T. L. Yaksh, Systemic TAK-242 prevents intrathecal LPS evoked hyperalgesia in male, but not female mice and prevents delayed allodynia following intraplantar formalin in both male and female mice, role of TLR4 in the evolution of a persistent pain state, *Brain, Behav., Immun.*, 2016, **56**, 271–280.

45 S. E. Hussey, H. Liang, S. R. Costford, A. Klip, R. A. DeFronzo, A. Sanchez-Avila, B. Ely and N. Musi, TAK-242, a small-molecule inhibitor of Toll-like receptor 4 signalling, unveils similarities and differences in lipopolysaccharide- and lipid-induced inflammation and insulin resistance in muscle cells, *Biosci. Rep.*, 2012, **30**, 37–47.

46 S. Oya, Y. Yokoyama, T. Kokuryo, M. Uno and K. Yamauchi, Nagino M Inhibition of Toll-like receptor 4 suppresses liver injury induced by biliary obstruction and subsequent intraportal lipopolysaccharide injection, *Am. J. Physiol.: Gastrointest. Liver Physiol.*, 2014, **306**, 244–252.

47 K. C. Li, Y. L. Ho, W. T. Hsieh, S. S. Huang, Y. S. Chang and G. J. Huang, Apigenin-7-Glycoside Prevents LPS-Induced Acute Lung Injury *via* Downregulation of Oxidative Enzyme Expression and Protein Activation through Inhibition of MAPK Phosphorylation, *Int. J. Mol. Sci.*, 2015, **16**, 1736–1754.

48 Q. Gong, H. Yin, M. Fang, Y. Xiang, C. L. Yuan, G. Y. Zheng, H. Yang, P. Xiong, G. Chen and F. L. Gong, Heme oxygenase-1 upregulation significantly inhibits TNF-α and Hmgb1 releasing and attenuates lipopolysaccharide-induced acute lung injury in mice, *Int. Immunopharmacol.*, 2008, **8**, 792–798.

49 J. C. Wataha, J. B. Lewis, V. V. McCloud, M. Shaw, Y. Omata, P. E. Lockwood, R. L. Messer and J. M. Hansen, Effect of mercury(II) on Nrf2, thioredoxin reductase-1 and thioredoxin-1 in human monocytes, *Dent. Mater.*, 2008, **24**(6), 765–772.

50 V. Sueblinvong, S. T. Mills, D. C. Neujahr, Y. M. Go, D. P. Jones and D. M. Guidot, Nuclear Thioredoxin-1 Overexpression Attenuates Alcohol-Mediated Nrf2 Signaling and Lung Fibrosis, *Alcohol.: Clin. Exp. Res.*, 2016, **40**(9), 1846–1856.